



MIT Open Access Articles

Oral delivery of systemic monoclonal antibodies, peptides and small molecules using gastric auto-injectors

The MIT Faculty has made this article openly available. **Please share** how this access benefits you. Your story matters.

Citation	Abramson, Alex, Frederiksen, Morten Revsgaard, Vegge, Andreas, Jensen, Brian, Poulsen, Mette et al. 2021. "Oral delivery of systemic monoclonal antibodies, peptides and small molecules using gastric auto-injectors." Nature Biotechnology, 40 (1).
As Published	10.1038/S41587-021-01024-0
Publisher	Springer Science and Business Media LLC
Version	Author's final manuscript
Citable link	https://hdl.handle.net/1721.1/141391
Terms of Use	Creative Commons Attribution-Noncommercial-Share Alike
Detailed Terms	http://creativecommons.org/licenses/by-nc-sa/4.0/

Title: Oral delivery of systemic monoclonal antibodies, peptides and small molecules using gastric auto-injectors

Authors: Alex Abramson^{1,*,§}, Morten Revsgaard Frederiksen^{2,#,§}, Andreas Vegge^{3,§}, Brian Jensen², Mette Poulsen², Brian Mouridsen², Mikkel Oliver Jespersen², Rikke Kaae Kirk³, Jesper Windum², František Hubálek⁴, Jorrit J. Water⁴, Johannes Fels⁴, Stefán B Gunnarsson⁴, Adam Bohr⁴, Ellen Marie Straarup³, Mikkel Wennemoes Hvitfeld Ley², Xiaoya Lu^{1,&}, Jacob Wainer^{1,%}, Joy Collins¹, Siddartha Tamang¹, Keiko Ishida^{1,9}, Alison Hayward^{1,9}, Peter Herskind², Stephen T. Buckley⁴, Niclas Roxhed^{1,6}, Robert Langer^{1,5,7}, Ulrik Rahbek^{4*}, Giovanni Traverso^{1,8,9*}

Affiliations:

¹Department of Chemical Engineering and David H. Koch Institute for Integrative Cancer Research, Massachusetts Institute of Technology, Cambridge, MA 02139

²Devices and Delivery Solutions, Novo Nordisk A/S, Hilleroed, Denmark

³Global Drug Discovery, Novo Nordisk A/S, Maaloev, Denmark

⁴Global Research Technologies, Novo Nordisk A/S, Maaloev, Denmark

⁵Institute for Medical Engineering and Science, Massachusetts Institute of Technology, Cambridge, MA 02139

⁶Department of Micro and Nanosystems, KTH Royal Institute of Technology, Stockholm, Sweden.

⁷Media Lab, Massachusetts Institute of Technology, Cambridge, MA 02139

⁸Department of Mechanical Engineering, Massachusetts Institute of Technology, Cambridge, MA 02139

⁹Division of Gastroenterology, Brigham and Women's Hospital, Harvard Medical School, Boston, MA 02115

[§]Contributed equally to this work

*Correspondence to: ulyr@novonordisk.com, cgt20@mit.edu

Present Address:

[†]Department of Chemical Engineering, Stanford University, Stanford, CA 94305-5025, USA.

[#]Orbex Denmark, Copenhagen, Denmark.

[&]Department of Biomedical Engineering, Johns Hopkins University, Baltimore, MD, 21218, USA.

[%]Fractyl Laboratories Inc., Lexington, MA, 02421, USA.

Abstract:

Oral administration provides a simple and non-invasive approach for drug delivery. However, due to poor absorption and swift enzymatic degradation in the gastrointestinal tract, a wide range of molecules must be parenterally injected to attain required doses and pharmacokinetics. Here we present an orally dosed liquid auto-injector capable of delivering up to 4-mg doses of bioavailable drug with the rapid pharmacokinetics of an injection, reaching an absolute bioavailability of up to 80% and a maximum plasma drug concentration within 30 min after dosing. This approach improves dosing efficiencies and pharmacokinetics an order of magnitude over our previously designed injector capsules and up to two orders of magnitude over clinically available and preclinical chemical permeation enhancement technologies. We administered the capsules to swine for delivery of clinically relevant doses of four commonly injected medications, including adalimumab, a GLP-1 analog, recombinant human insulin and epinephrine. These multi-day dosing experiments and oral administration in awake animal models support the translational potential of the system.

Main Text:

Introduction

Biologic drugs are generally regarded as one of the most efficacious modalities for the treatment of a range of disease such as diabetes^{1,2} and Crohn's disease³. Nevertheless, their injection-based method of administration often causes healthcare professionals to delay their initiation in favor of less effective oral medications^{4,5}. Patients widely prefer pills over injections and report significant negative impacts to their quality of life when prescribed an injectable medication⁶. Thus, a method for the oral administration of a broad range of biologic drugs could revolutionize treatment strategies for many diseases.

Recently, significant advancements have been demonstrated in oral biologic drug delivery⁷⁻¹⁰, yet these new technologies suffer from limited drug loading, reduced systemic bioavailability, and/or delayed pharmacokinetics compared to their parenterally dosed counterparts. These limitations prevent the use of such technologies for the oral delivery of widely used drugs such as adalimumab and pre-prandial insulin. For example, chemical enhancers like salcaprozate sodium (SNAC) have been shown to facilitate transport of semaglutide, a glucagon-like peptide-1 receptor agonist (GLP-1 RA), across the gastric mucosa with an oral bioavailability of approximately 1%¹¹⁻¹³. This oral formulation of semaglutide (tradename Rybelsus®) recently received approval by the U.S. Food and Drug Administration, the European Medicines Agency, and the Pharmaceuticals and Medical

Devices Agency of Japan. While semaglutide is a potent molecule, as reflected by subcutaneous dosing as low as 0.5 mg per week, the modest oral bioavailability achieved by SNAC-based formulations makes such approaches less suitable as cost-effective treatments for molecules of lower potency like insulin and adalimumab^{14,15}. Additionally, a range of approaches for oral biologic delivery are in early development^{7-10,16-20}, with examples including capsule-based microneedle devices²¹⁻²⁴, ionic liquids^{25,26}, and microparticles or nanoparticles^{27,28}. While collectively these technologies are promising, further preclinical and clinical validation as well as development to accommodate doses on the therapeutically relevant milligram scale remain to be demonstrated for many of these systems.

Previously, we reported on two orally dosed devices, the SOMA²¹ and LUMI²² capsules, capable of systemically delivering solid formulations of macromolecule drugs with high bioavailabilities via injections to the stomach and small intestine respectively. These devices, while able to consistently perform as described, suffered from key limitations: low dosing sizes on the order of 300 – 700 µg per pill; delayed or zero order kinetic drug delivery rates that limited their absolute bioavailability to 10% or less during the first 3.5 hours after actuation; and the requirement for gastrointestinal fluid, filled with degradative enzymes, to interact with the drug formulation for a short period of time before tissue wall injection. These constraints prevented the pills from delivering drugs with large dosage requirements like adalimumab as well as drugs that require fast action such as mealtime insulin or epinephrine.

Here we report a new version of our SOMA device which solves these challenges by using redesigned actuation and delivery systems (Figure 1 a). Our new pill can achieve multi-milligram doses of drugs ranging in size from small molecules to monoclonal antibodies (Figure 1b). The pill achieves a maximum drug plasma concentration comparable in magnitude to the standard-of-care subcutaneous injection as quickly as 30 minutes after dosing and delivers with a calculated absolute bioavailability of up to 80% within a timespan of hours.

Results

An orally dosed capsule for gastric injections of liquid formulations

To orally deliver multi-milligram doses across a range of drugs which today require injection, we developed an ingestible pill capable of systemically delivering liquid formulations of pharmaceuticals via an injection into the gastric submucosa. We recognized the potential of liquid injections to readily distribute within the stomach's submucosal plane, thereby accommodating larger dosing volumes than solid dosage forms. Additionally, the increased surface area of interaction between the formulation and the tissue when compared to a solid dose pellet enables accelerated drug pharmacokinetics and pharmacodynamics. Moreover, by targeting the stomach rather than the small intestine, the capsule circumvents the 1-4 hours required for gastric emptying^{24,29} and delivers its payload minutes after ingestion. The 4-6 mm thick stomach wall tissue, compared to the 0.1-2 mm thick small intestine wall³⁰, also provides a greater safety margin to mitigate the risk of a complete thickness tissue perforation during injection. Furthermore, while capsules delivering solid dosage forms^{11,21-23} must rely on the solid state properties of the drug, such as its ability to be compressed, the liquid formulations in this study are similar to pre-approved and pre-tested parenteral formulations. Long term stability studies for liquid drug formulations loaded in the L-SOMA device are presented in Extended Data figure 1. Taking these factors into account, a liquid injection based drug delivery method can effectively enable the delivery of fast-acting, large-dose pharmaceuticals.

The liquid-injecting self-orienting millimeter-scale applicator (L-SOMA), a 12 mm in diameter and 15 mm tall capsule, utilizes a self-orienting geometry that autonomously positions the device so that its injection mechanism always faces towards the tissue wall^{21,31}. A weighted bottom and a hollow shell that mirrors the geometry of a self-righting tortoise enables the device to reorient itself on the stomach wall in the same manner that a weeble-wobble toy rights itself after being disturbed. The design ensures that the capsule delivers the dose into the tissue rather than the gastric cavity, generating a submucosal depot and circumventing enzymatic degradation that occurs in the lumen⁹.

To deliver the drug, the L-SOMA uses a staged and sequence controlled multi-spring actuation system that injects a hypodermic needle beneath the gastric mucosa and thereupon delivers 80 μ L of liquid drug formulation

into the submucosal space. The L-SOMA's actuation mechanism is located on the shell of the device, eliminating the need for gastric fluid to enter the pill and be in contact with the loaded drug before injection. A dissolving pellet, accessed through a hole on the top of the pill, holds an injection molded needle hub in place using a latching mechanism (Figure 1 c, Extended Data Fig. 2). Over time this pellet dissolves, releasing the latches as they move inwards into the void where the pellet previously sat. Because the actuation mechanism places the stress from the compressed springs on the plastic top rather than the dissolving hub, we can load springs with a higher relative compression force. This increased power enables a distance-limited, rather than force-limited, penetration event, allowing the device to more accurately target a given tissue layer. Once actuated, the L-SOMA first inserts a needle into the tissue to a defined distance using an excess of force. Then it uses a second spring to push down on a plunger which drives the liquid drug formulation through the needle and into the gastric submucosa (Figure 1 d-g). Two membranes seal off the dose storage area and prevent leakage as the plunger pushes the liquid through a side hole in the needle and out via the needle's tip (Extended Data Fig. 2). By decoupling the needle insertion from the liquid injection, the device achieves delivery of its entire dose deep within the tissue instead of releasing the dose as the needle moves through the tissue (Figure 1 f-u). Therefore, this staged injection system prevents any of the dose from expelling into the gastric fluid where it could be degraded.

We studied the optimal needle penetration depth required to target the stomach submucosa for delivery by characterizing injections of contrast dye to pre-defined depths in ex vivo swine stomach tissue (Figure 1h-p, Extended Data Fig. 3). Using MicroCT imaging, we calculated the percent of liquid remaining in the tissue after dosing to a given depth (Figure 1q). We observed that for 3 mm and 4 mm needle injection depths, the dose sometimes delivered into the mucosa rather than the submucosa. Because the mucosa cannot accept as much liquid as the submucosa, a large proportion of the dye leaks out of the tissue during these misfires. By extending the needle insertion depth to 4.5 mm or greater, the device consistently delivered the entire liquid dose into the tissue and experienced no leakage. At deeper injection depths, injections into the outer muscle layer of the stomach tissue occurred at a rate of 2/12, 4/12, and 1/4 for insertion depths of 4.5 mm, 5 mm and 6 mm respectively.

However, complete dose delivery into the tissue was confirmed in these cases, providing confidence that a muscular injection would not affect the delivered drug dose.

In addition to studying penetration depth, we also examined the effects of the needle grind on the force required for fluid injection. We noted that lower angle grinds facilitated fluid delivery compared to flatter tips (Extended Data Fig. 3). Guided by this data, we designed an L-SOMA device which inserted a 10° grind needle to a depth of 4.5 mm, thereby reducing the perforation risk compared to deeper injection depths while ensuring maximal delivery into the tissue. Ex vivo experiments (Figure 1m-p) with L-SOMA devices revealed that needles of these dimensions reliably targeted the submucosa and delivered their entire payload into the tissue. Histology from ex vivo experiments on swine and dog stomachs as well as histology taken from swine dosed in vivo using the L-SOMA confirmed that the device delivered its entire payload and that the needle did not perforate the tissue (Figure 2a-e, 2g-k, and Extended Data Fig. 4).

A retractable needle system for gastric injections

To mitigate the potential risk of an exposed needle in the gastrointestinal tract during device passage, we designed an L-SOMA capable of retracting the needle into the device after injection (Extended Data Fig. 5). We designed an L-SOMA device with a third spring and a second dissolving pellet which subsequently actuated after drug injection. As measured through in vitro experiments on a texture analyzer, needle retraction required less than 1 mN of force to overcome the friction from the tissue and an additional 1N of force to overcome the friction at the septum-needle interface. MicroCT images captured the needle retraction event during ex vivo tests on swine stomach tissue (Figure 1 r-u, and see Supplementary Video S1), and we confirmed needle retraction during in vivo swine experiments via visualization through endoscopy and fluoroscopy (see Supplementary Video S2). While sharp objects under 1 cm, including needles, have previously been shown to have the capacity to transit safely through the GI tract³²⁻³⁴, and experiments we and others performed using devices with exposed sharp objects provided evidence that devices could safely pass through the gastrointestinal tract with an exposed needle^{21,22,33-35}, the

needle retraction system provides an additional safety measure to reduce the risk of intestinal injury during device passage.

Delivering clinically relevant doses of adalimumab, insulin, GLP-1, and epinephrine in large animals

We performed in vivo swine experiments in which we dosed L-SOMA devices loaded with either 4 International Units (0.14 mg) of recombinant human insulin, 4 mg of an inactivated semaglutide-like GLP-1 analog, 4 mg of the monoclonal antibody adalimumab, or 0.24 mg of the small molecule epinephrine (Figure 3). An inactivated semaglutide-like molecule was used to prevent adverse reactions due to potentially high exposure. L-SOMA dosings were compared to subcutaneous or intramuscular dosings as positive controls.

Using an endoscope, we placed L-SOMA devices into swine stomachs and allowed them to independently actuate. Actuation occurred within $4:05 \pm 1:17$ minutes (Mean \pm SD, n=8). After either 15 minutes or 2 hours, the devices were removed from the animal, and the animals' anesthesia were reversed. Uptake profiles for swine only anaesthetized for 15 minutes demonstrated faster pharmacokinetics and higher C_{max} values compared to the uptake profiles for swine anaesthetized for two hours. In either case, within 15 minutes after L-SOMA administration of insulin, inactivated GLP-1, or epinephrine, plasma exposure of drug was observed. Adalimumab was observed in the serum within one hour after L-SOMA administration. Insulin dosed swine experienced immediate hypoglycemic onset (Figure 3b, f), and epinephrine dosed swine experienced a rapid rise in heart rate (Figure 3 k, n) and blood glucose (Extended Data Fig. 6) in both the injection and L-SOMA experimental groups. We analyzed H&E stained histology from the epinephrine dosed swine to assess the effects of the drug on the tissue (see Extended Data Fig. 7). Swine dosed with adalimumab or inactivated GLP-1 using either L-SOMA capsules or subcutaneous injections displayed measurable plasma drug levels for at least 3 days after dosing, consistent with the drugs' half-lives. Moreover, we dosed three swine with insulin loaded L-SOMA devices on three subsequent days, and all swine showed repeated and consistent systemic uptake and subsequent plasma glucose drops over the dosing period (Figure 3 o, p).

In total, 28 of the 31 L-SOMA-dosed swine demonstrated systemic uptake, leading to a positive dosing rate of over 90%. Devices that did not deliver drug either experienced an actuator malfunction or the drug was not taken up into the animal's bloodstream.

The exposure profiles in figure 3 show completely comparable exposures between L-SOMA dosing and subcutaneous or intramuscular dosing for compounds ranging from small molecules to monoclonal antibodies. Bioavailabilities derived from L-SOMA and subcutaneous dosing of insulin and GLP-1 analog were calculated. L-SOMA dosed insulin demonstrated a $51 \pm 16\%$ (SD) bioavailability over a two-hour sampling period (Range = 30% - 81%, n=7). This compared to a $57 \pm 8\%$ (SD) bioavailability for the swine dosed with insulin subcutaneously (Range = 51% - 66%, n=3). The bioavailability of L-SOMA dosed GLP-1 analog over a three-day sampling period was $103 \pm 42\%$ (SD) (Range = 55% - 135%, n=3) when excluding an L-SOMA which showed 0% uptake after actuation in the stomach and $78 \pm 62\%$ when including this extra data point. This compared to a $78 \pm 4\%$ (SD) bioavailability for subcutaneously dosed GLP-1 analog (Range = 75.6% - 82.5%, n=3). Absolute bioavailability was calculated based on i.v. profiles obtained in a separate group of animals with comparable age; however, differences may be observed in disposition kinetics and additionally, the long $t_{1/2}$ of GLP-1 necessitates a high degree of extrapolation. Both methodological details could explain the >100% bioavailability observed for GLP-1. Collectively, we observed exposure levels on par with subcutaneous or intramuscular dosing for all tested compounds.

We compared the drug uptake profiles from L-SOMA injection with uptake profiles from swine dosed with these drugs without an intragastric injection. For both epinephrine and adalimumab, endoscopic gavage experiments with an equivalent drug load to the L-SOMA were performed on swine as negative controls, and negligible uptake was observed (Extended Data Fig. 8). Previously published results on insulin²¹ and GLP-1¹¹ demonstrate their severely limited ability to traverse the stomach lining for systemic uptake when administered without a permeation enhancer or physical permeation enhancing device, and a bioavailability of approximately

1% is observed when using a permeation enhancer¹¹. Compared to these control studies, the L-SOMA is capable of delivering larger systemic doses of drugs.

Assessing the safety and feasibility of multi-day dosing

After dosing, we either monitored the animals for one week or euthanized the animals and performed histological studies. All animals maintained their normal behavior and eating patterns after dosing. Endoscopic observation immediately following delivery revealed that some animals showed minor bleeding after L-SOMA administration, but this bleeding stopped within minutes. No blood in the stool was observed. No abnormalities were seen in H&E stained histology samples taken from the injection site within two hours after dosing (Figure 2 d, e, j, k and Extended Data Fig. 7). In the three swine that were dosed on multiple occasions over three days, we collected tissue samples from the cardia, the fundus, and the pyloric region after euthanasia through standard histological procedures. We noted no abnormalities from dosing (Extended Data Fig. 9a-c). In addition to standard histopathological sampling, we inspected the serosal and mucosal surfaces of the swine dosed multiple times and noted a single mucosal abnormality on two of the three swine. The focal lesion from the fundic region observed in the first swine showed a minimal acute superficial hemorrhage with intact epithelial lining (Figure 2 f, l). The focal lesion observed in the second swine showed acute minimal erosion with sloughing of epithelial cells and peripheral acute hemorrhage (Extended Data Fig. 9d-e). The first lesion is most likely related to the L-SOMA needle injection that occurred a day prior to euthanasia and tissue sampling, whereas the second lesion observed is most likely a mechanical trauma caused by the endoscope when dosing the animal and as such is not a direct effect of the intended L-SOMA dosing. Because we did not find macroscopic abnormalities on every swine and we did not find any abnormalities from devices dosed more than one day before euthanasia, these findings suggest that some L-SOMA devices may generate minimal tissue damage that heals rapidly.

While the above experiments utilized an endoscope to assist in device delivery, we also performed experiments where we naturally orally dosed devices to awake dogs (n=8). These oral dosing experiments utilized

a different version of the SOMA concept than the L-SOMA and did not contain a drug formulation, but the size and density distribution is similar between the two pills. All animals effortlessly ingested the capsule. Through radiograph monitoring (Extended Data Fig. 10), we observed that the capsule reached the stomach, activated, and subsequently passed completely through the gastrointestinal tract as expected.

Discussion

In this paper, we demonstrated the L-SOMA pill's ability to dose four different pharmaceuticals with a broad range of molecular weights, half-lives, pharmacodynamic effects and dose requirements. The L-SOMA capsule facilitates a rapid pharmacokinetic uptake within minutes after administration and possesses a loading capacity of up to 4 mg of bioavailable drug, enabling the compatibility of this capsule with a new set of medications that could not previously be orally delivered.

Further device optimization, including a reduction in capsule size and an increase in drug loading could facilitate device ingestion and drug delivery as well as further mitigate risk of gastrointestinal obstruction. Current FDA approved daily dosed non-degradable drug delivery pills such as the 9 mm in diameter OROS capsule provide important guidance for device size, as they generate obstructions at a rate of just 1 in 29 million³⁶. Moreover, dosing drugs in the L-SOMA with wide therapeutic windows could mitigate the larger error associated with drug bioavailability in the pills compared to subcutaneous dosing.

Additional clinical experiments must be performed to assess how patients react to the pill. These experiments should include subjects varying in age, weight, height, diet, and disease status to understand the effects of anatomic and pathophysiologic variables on device actuation. While our initial multiday dosing studies did not demonstrate any evidence of the development of major stomach tissue abnormalities from L-SOMA injection, successful human translation will require longer repeated dosing regimens in preclinical and clinical models followed by characterization of injection sites. Additionally, it will require dosing in humans to monitoring for any adverse events including pain and tissue damage, in particular damage compromising the wall of the viscera.

As a comparison, 25 gauge Carr-Locke needle injections performed during endoscopy utilize a needle with a diameter twice as large as the L-SOMA needle and deliver more than 12x the liquid dose of the L-SOMA, and the traumas generated by these injections heal rapidly and rarely generate complications³⁷. Moreover, retrospective medical studies and experimental studies in large animal models on ingested sharp objects demonstrate the low risk of complications associated with sharp objects less than 1 cm in length^{22,33-35,38}. Nevertheless, further studies in humans are necessary to inform the safety and efficacy of the L-SOMA.

Here, we show that the L-SOMA can carry and deliver a broad range of drugs across a range of molecular weights via an oral capsule. In doing so, it can provide a less intrusive route of administration for drugs that are otherwise limited to injectables, presenting a route towards higher quality of life among patients^{6,15} with potentially higher adherence rates and ultimately, a potential improvement in clinical outcomes.

References:

1. Pratley, R. E. *et al.* Liraglutide versus sitagliptin for patients with type 2 diabetes who did not have adequate glycaemic control with metformin: a 26-week, randomised, parallel-group, open-label trial. *Lancet* **375**, 1447–1456 (2010).
2. Turner, R. C., Cull, C. A., Frighi, V., Holman, R. R. & Group, for the U. P. D. S. (UKPDS). Glycemic Control With Diet, Sulfonylurea, Metformin, or Insulin in Patients With Type 2 Diabetes Mellitus Progressive Requirement for Multiple Therapies (UKPDS 49). *JAMA* **281**, 2005–2012 (1999).
3. Colombel, J. F. *et al.* Adalimumab for Maintenance of Clinical Response and Remission in Patients With Crohn's Disease: The CHARM Trial. *Gastroenterology* **132**, 52–65 (2007).
4. Rubino, A., McQuay, L. J., Gough, S. C., Kvasz, M. & Tennis, P. Delayed initiation of subcutaneous insulin therapy after failure of oral glucose-lowering agents in patients with Type 2 diabetes: a population-based analysis in the UK. *Diabet. Med.* **24**, 1412–1418 (2007).
5. Ruemmele, F. M. *et al.* Consensus guidelines of ECCO/ESPGHAN on the medical management of pediatric Crohn's disease. *J. Crohn's Colitis* **8**, 1179–1207 (2014).
6. Boye, K. S. *et al.* Utilities and disutilities for attributes of injectable treatments for type 2 diabetes. *Eur. J. Heal. Econ.* **12**, 219–230 (2011).
7. Ahadian, S. *et al.* Micro and nanoscale technologies in oral drug delivery. *Advanced Drug Delivery Reviews* (2020) doi:10.1016/j.addr.2020.07.012.
8. Drucker, D. J. Advances in oral peptide therapeutics. *Nat. Rev. Drug Discov.* (2019) doi:10.1038/s41573-019-0053-0.
9. Anselmo, A. C., Gokarn, Y. & Mitragotri, S. Non-invasive delivery strategies for biologics. *Nat. Rev. Drug*

Discov. **18**, 19–40 (2018).

10. Brayden, D. J. & Alonso, M.-J. Oral delivery of peptides: opportunities and issues for translation. *Adv. Drug Deliv. Rev.* **106**, 193–195 (2016).
11. Buckley, S. T. *et al.* Transcellular stomach absorption of a derivatized glucagon-like peptide-1 receptor agonist. *Sci. Transl. Med.* **10**, eaar7047 (2018).
12. Pratley, R. *et al.* Oral semaglutide versus subcutaneous liraglutide and placebo in type 2 diabetes (PIONEER 4): a randomised, double-blind, phase 3a trial. *Lancet* **394**, 39–50 (2019).
13. Husain, M. *et al.* Oral Semaglutide and Cardiovascular Outcomes in Patients with Type 2 Diabetes. *N. Engl. J. Med.* **381**, 841–851 (2019).
14. Halberg, I. B. *et al.* Efficacy and safety of oral basal insulin versus subcutaneous insulin glargine in type 2 diabetes: a randomised, double-blind, phase 2 trial. *Lancet Diabetes Endocrinol.* **7**, 179–188 (2019).
15. Abramson, A., Halperin, F., Kim, J. & Traverso, G. Quantifying the Value of Orally Delivered Biologic Therapies: A Cost-Effectiveness Analysis of Oral Semaglutide. *J. Pharm. Sci.* **108**, 3138–3145 (2019).
16. Mahmood, A. & Bernkop-Schnürch, A. SEDDS: A game changing approach for the oral administration of hydrophilic macromolecular drugs. *Advanced Drug Delivery Reviews* vol. 142 91–101 (2019).
17. Phan, T. N. Q., Shahzadi, I. & Bernkop-Schnürch, A. Hydrophobic ion-pairs and lipid-based nanocarrier systems: The perfect match for delivery of BCS class 3 drugs. *Journal of Controlled Release* vol. 304 146–155 (2019).
18. Fox, C. B. *et al.* Fabrication of Sealed Nanostraw Microdevices for Oral Drug Delivery. *ACS Nano* **10**, 5873–5881 (2016).
19. Banerjee, A., Wong, J., Gogoi, R., Brown, T. & Mitragotri, S. Intestinal micropatches for oral insulin delivery.

J. Drug Target. **25**, 608–615 (2017).

20. Melmed, S. *et al.* Safety and efficacy of oral octreotide in acromegaly: Results of a multicenter phase III trial. *J. Clin. Endocrinol. Metab.* **100**, 1699–1708 (2015).
21. Abramson, A. *et al.* An ingestible self-orienting system for oral delivery of macromolecules. *Science* (80-.). **363**, 611–615 (2019).
22. Abramson, A. *et al.* A luminal unfolding microneedle injector for oral delivery of macromolecules. *Nat. Med.* **25**, 1512–1518 (2019).
23. Hashim, M. *et al.* Jejunal wall delivery of insulin via an ingestible capsule in anesthetized swine—A pharmacokinetic and pharmacodynamic study. *Pharmacol. Res. Perspect.* **7**, e00522 (2019).
24. AK, D. *et al.* A robotic pill for oral delivery of biotherapeutics: safety, tolerability, and performance in healthy subjects. *Drug Deliv. Transl. Res.* (2021) doi:10.1007/S13346-021-00938-1.
25. Banerjee, A. *et al.* Ionic liquids for oral insulin delivery. *Proc. Natl. Acad. Sci. U. S. A.* **115**, 7296–7301 (2018).
26. Angsantikul, P. *et al.* Ionic Liquids and Deep Eutectic Solvents for Enhanced Delivery of Antibodies in the Gastrointestinal Tract. *Adv. Funct. Mater.* 2002912 (2020) doi:10.1002/adfm.202002912.
27. Mathiowitz, E. *et al.* Biologically erodable microspheres as potential oral drug delivery systems. *Nature* **386**, 410–414 (1997).
28. Lamson, N. G., Berger, A., Fein, K. C. & Whitehead, K. A. Anionic nanoparticles enable the oral delivery of proteins by enhancing intestinal permeability. *Nat. Biomed. Eng.* **4**, 84–96 (2020).
29. Bolondi, L. *et al.* Measurement of gastric emptying time by real-time ultrasonography. *Gastroenterology* **89**, 752–759 (1985).

30. Derrickson, B. H. & Tortora, G. J. *Principles Of Anatomy And Physiology*. (Wiley, 2008).
31. Várkonyi, P. L. & Domokos, G. Mono-monostatic Bodies: The Answer to Arnold's Question. *Math. Intell.* **28**, 34–38 (2006).
32. Butterworth, J. R., Wright, K., Boulton, R. A., Pathmakanthan, S. & Goh, J. Management of swallowed razor blades - Retrieve or wait and see? *Gut* **53**, 475–477 (2004).
33. Velitchkov, N. G., Grigorov, G. I., Losanoff, J. E. & Kjossev, K. T. Ingested foreign bodies of the gastrointestinal tract: Retrospective analysis of 542 cases. *World J. Surg.* **20**, 1001–1005 (1996).
34. Traverso, G. *et al.* Microneedles for drug delivery via the gastrointestinal tract. *J. Pharm. Sci.* **104**, 362–7 (2015).
35. Webb, W. A. Management of foreign bodies of the upper gastrointestinal tract: Update. *Gastrointest. Endosc.* **41**, 39–51 (1995).
36. Bass, D. M., Prevo, M. & Waxman, D. S. Gastrointestinal safety of an extended-release, nondeformable, oral dosage form (OROS): a retrospective study. *Drug Saf.* **25**, 1021–1033 (2002).
37. Ben-Menachem, T. *et al.* Adverse events of upper GI endoscopy. *Gastrointest. Endosc.* **76**, 707–718 (2012).
38. Ginsberg, G. G. Management of ingested foreign objects and food bolus impactions. *Gastrointest. Endosc.* **41**, 33–38 (1995).
39. Coffman, C. *et al.* Particles comprising a therapeutic or diagnostic agent and suspensions and methods of use thereof. (2017).
40. Savjani, K. T., Gajjar, A. K. & Savjani, J. K. Drug Solubility: Importance and Enhancement Techniques. *ISRN Pharm.* **2012**, 1–10 (2012).

Acknowledgements: We thank J. Haupt, M. Jamiel, C. Cleveland, C. Anker, A. Benfeldt, C. Jensen, H. Toftelund, and A.H. Uhrenfeldt for help with in vivo porcine work. We thank the MIT Koch Institute Swanson Biotechnology Center histology and high throughput cores for technical support. We thank U. Stilz, T. Kjeldsen, L.F. Iversen, M. Bielecki and P.B. Nielsen, for discussions about SOMA development. We are grateful to all members of Langer and Traverso laboratories and Novo Nordisk for their expertise around biologic drug delivery. We thank the team at GTReel Productions, specifically Giancarlo Traverso, for assistance with assembly of the supplementary videos.

Funding: Work funded in part by: Novo Nordisk grant (R.L., G.T.), NIH Grant No. EB-000244 (R.L., G.T.), NSF GRFP fellowship (A.A.), Karl Van Tassel (1925) Career Development Professorship, Department of Mechanical Engineering, Massachusetts Institute of Technology and Division of Gastroenterology, Brigham and Woman's Hospital (G.T.), Viking Olof Björk scholarship trust (N.R.).

Author Contributions: A.A., M.R.F., R.L., G.T. developed concept. A.A., M.R.F., M.O.J., J. Windum, B.M., and B.J. designed the device. M.W.H.L. and M.P. performed injection characterization studies. A.A., J. Wainer, and X.L. performed high speed video experiments. A.A., A.V., E.M.S. J.C., S.T., K.I., and A.H. performed in vivo experiments. J.J.W. and A.B. developed liquid formulations and dissolving pellets. F.H. performed activity and stability assays on liquid formulations. J.F. S.B.G. and A.V. performed analysis on in vivo data. R.K.K. performed histology. U.R., S.T.B, P.H., N.R., R.L., G.T. had oversight and leadership responsibility for the research activity planning and execution. A.A., M.R.F., A.V., R.L. and G.T. wrote the manuscript. All authors discussed results and commented on the manuscript.

Competing interests: M.R.F., M.P., A.V., B.M., F.H., J.J.W., J.F., R.K.K., S.B.G., E.M.S., S.T.B., P.H., M.O.J., J. Windum, A.B., E.S., and U.R. are employees of Novo Nordisk. M.W.H.L. and B.J. are hired as consultants for Novo Nordisk. A.A., M.R.F., A.V., M.P., J.J.W., M.W.H.L., U.R., B.J., J. Windum, J. Wainer, X.L., N.R., G.T. and R.L. are co-inventors on patent applications describing oral biologic drug delivery. A.A., R.L. and G.T. report receiving consulting fees from Novo Nordisk. A.A. reports receiving consulting fees from Eli Lilly. Complete details of all relationships for

profit and not for profit for G.T. can found at the following link: <https://www.dropbox.com/sh/szi7vnr4a2ajb56/AABs5N5i0q9AfT1IqJAE-T5a?dl=0>. For a list of entities with which R.L. is involved, compensated or uncompensated, see: www.dropbox.com/s/yc3xqb5s8s94v7x/Rev%20Langer%20COI.pdf?dl=0

Data Availability: The data used to generate the figures and numerical statistics in this paper can be found as attached excel files in the Supplementary Information.

Materials and methods:

Acquisition of ex vivo stomach tissue

All studies involving animals were approved by and performed in accordance with the Committee on Animal Care at MIT and the Novo Nordisk Environment and Bioethics Committee. Swine stomach tissue was acquired from LYD pigs (landrace, Yorkshire or Duroc) housed at Novo Nordisk facilities in Ganløse, DK. The swine were sacrificed 2-4 hours before the experiments, and the stomachs were stored in a PBS solution until running the tests. The test samples were cut from the anterior wall and the greater curvature into approximately 5 cm by 5 cm pieces. The tissue sample was placed in a small standard hard acrylic dish. Ex vivo Yorkshire swine tissue procured for research performed at MIT was obtained from the Blood Farm (West Groton, USA) and transported to the lab on ice. The tissue was used within 24 hours after euthanizing the animal.

Histology

Swine stomach tissue was fixed in 10 % buffered formalin for a minimum of 24 hours, processed in a tissue processor (ASP300S, Leica, USA), embedded in paraffin and cut at 3 μ m thickness. Paraffin sections were stained histochemically with haematoxylin and eosin (H&E) and immunohistochemically using antibodies raised against alpha smooth muscle actin (Rb-anti-SMA, #ab5694, Abcam) and insulin (Mo-anti-insulin, #HUI-018, in-house).

L-SOMA Manufacturing

Device tops were fabricated using a ProJet 6000HD SLA printer (3D systems, Rock Hill, USA) and VisiJet SL Flex ink (3D systems). Device bottoms were fabricated with 304 stainless steel on a CTX 310 ecoline lathe (DMG Mori, Nakamura-ku, Japan). Needle hubs made from polyoxymethylene and plungers made from polyphenylene ether and thermoplastic elastomer Kraiburg were injection molded by Insign (Struer, Denmark). A spring with a 4.7 N maximum loading force used to insert the needle and a spring with an 8.6 N maximum loading force used to inject the liquid dose were custom made for the L-SOMA by Madsen Fjederfabrik (Brøndbyvester, Denmark). The 4.7 N spring was 3.75 mm in height in its compressed state, had a spring constant of 0.65 N/mm, and was 4.5 mm in diameter. The 8.6 N spring was 3.90 mm in height in its compressed state, had a spring constant of 0.53 N/mm, and was 8.7 mm in diameter. The springs were made from 18-8 stainless steel. The silicone encapsulation used to hold the dose was molded using a 3D printed SLS mold from Elastosil 4542B (Wacker Chemie, Munich, Germany). A 32 G Novo fine needle cut to protrude 4.5 mm out of the device was also used. A single side hole in the needle was milled out to allow for the liquid pharmaceutical formulation to flow out of the device. The pellet actuators were made from isomalt (Biosynth, Itasca, USA), and they were prepared in dimensions ranging from 0.8-1.2 mm in diameter via compression. All device pieces were placed inside of the top and bottom encapsulation parts and pressed together to form the L-SOMA device. Once pressed together, the top encapsulation piece was secured in place via an internal locking mechanism. The entire device measured 12 mm in diameter and 15 mm in height. The top of the retractable L-SOMA was 3D printed on a 3D Systems Model 4 Modular Base Unit using Pro Black 10 ink, and it was cured in an LC-3DPrintBox for 90 minutes (Rock Hill, USA). The retractable version of the L-SOMA used in this paper possesses an extra spring and an extra dissolving plug. To incorporate these pieces in a proof-of-concept device, we used a device that was 67% larger in diameter.

An important consideration for the L-SOMA design is the ability to scale up the manufacturing process to accommodate the fabrication of millions of devices. The device top, the needle hub, the plunger and the silicone encapsulation can all be injection molded, a process allowing for mass production. The bottom of the device is currently fabricated using a lathe in a process that can also be scaled-up. The springs, although requiring custom

specifications, can be fabricated *en masse* during scale-up. The needle production can also be scaled up; creating the side hole in the needle will require an extra fabrication step compared to traditional needle manufacturing, but this process is already performed at high volumes to produce Whitacre needles. Assembly of the system can be broken up into three steps: device top assembly, device drug loading, and the assembly of the top and bottom pieces. Currently, the drug is loaded manually, generating error in drug loading, but this process could be automated in the future. Because the L-SOMA contains more parts than the SOMA system, it may be more expensive to produce and more complicated to assemble. Nevertheless, the designs and components of the L-SOMA do allow for mass manufacturing using traditional manufacturing techniques.

Self-Orientation and Device Actuation:

L-SOMA devices were tested for self-orientation on ex vivo swine tissue by randomly dropping the device onto a piece of swine tissue measuring at least 5 cm x 5 cm from a height of at least 5 cm. The device was considered oriented if the hole used for the needle to pass through was in contact with the tissue.

The shape and density distribution of the device draws inspiration from the leopard tortoise, an animal with the ability to self-orient from any configuration. The device's high curvature upper portion coupled with its low center of mass ensures that it only possesses one stable orientation, defined as an angle in which the device's center of mass is at a local minimum. Additionally, the flat bottom of the L-SOMA stabilizes its preferred configuration and ensures that it does not tip over and misfire into the lumen if a patient moves about during actuation. We have previously demonstrated the robust self-righting nature of the shape when validating its ability to deliver solid dosage forms²¹; after changing the device to allow for liquid dosing, we retested the L-SOMA for self-orientation 300 times on ex vivo stomach tissue. The L-SOMA device oriented to its preferred configuration during every experiment in less than 1 second.

As soon as the L-SOMA is ingested, a hydration-based actuator plug made from isomalt begins to dissolve. The plug holds a hub connected to the injection needle in place. Once dissolved, the plug releases the hub and a compressed

spring expands to deliver the needle into the tissue. After a set distance, the hub is stopped by a tab on the encapsulation of the device. This ensures that the needle inserts a set distance into the tissue.

Ex vivo penetration depth studies

Needles were inserted into the swine stomach sample with the help of a custom fixture 3D printed from PA 2105 Nylon on an Formiga P110 SLS printer (EOS, Krailling, Germany) (see Extended Data Fig. 3). This fixture was able to fixate a standard 3 mL glass cartridge with a mounted 6 mm Novo Fine 32G needle (Novo Nordisk, DK). The inner nominal diameter of the cartridge was 9.25 mm. A piston rod was mounted on a LR5K Plus tensile tester (Lloyd Instruments, Bognor Regis, UK), Software NEXYGEN Plus v3.0 (Lloyd Instruments), and could then push down on the bromomethyl rubber plunger, thereby ejecting liquid. To ensure the correct penetration depth of the needle into the tissue, the fixture had pin holes at 1 mm height steps. Inserting a pin kept the cartridge and needle in place while loading a spring.

After loading the fixture spring, the needle tip was placed at the tissue surface. Releasing the pin caused the needle to be inserted rapidly with the pre-set penetration depth, minimizing any operator-specific dependencies. Needles were inserted 3.0 mm, 4.0 mm, 4.5 mm, 5.0 mm, and 6 mm into the tissue depending on the experiment. The ex vivo swine stomachs measured 7.0 ± 1.3 mm thick at the sites of injection.

Seven needles with different designs or properties were included in the study. Four of the needles were marketed needles with no modifications; NovoFine 32G (NF-32), NovoFine 28G (NF-28), NovoFine 27G (NF-27-B) where we used the single-grind back-end of the needle), and a Pencil Shape G29 needle with sidehole from Acti-Med (PS-29). NF-32 and NF-28 needles possessed backgrinds of 12.5 ± 2 degrees. NF-27-B needles possessed a backgrind of 28 ± 4 degrees. Two needles were marketed needles with custom grinds; NovoFine 30G (NF-30-B20) and NovoFine 30G (NF-30-B40). These had grinds of 20 ± 4 degrees and 40 ± 4 degrees respectively. This means the angle tips of the needles were 70 degrees and 50 degrees respectively. All Novo Fine needles were obtained from Novo Nordisk A/S, Bagsværd, Denmark. The NF-32 was used for the L-SOMA devices.

For the liquid we used insulin test media (Novo Nordisk, Copenhagen, Denmark) mixed with Iomeron 350 mg/mL contrast agent (Bracco, Milan, Italy) for CT scanning. The injected volume was 170 μ L, and the piston speed was set to 0.25 mm/s. The injection flow rate was 21 μ L/s. During the injection the force needed to inject the depot was measured. After each injection into the tissue an air shot was performed, where the needle ejected liquid out into free air to check for possible clogging. Of the 90 air shots in total, not one showed any sign of clogging.

After the depot injection, the tissue samples were scanned in a Nanotom S MicroCT scanner (Phoenix/GE, Boston, USA). We used the accompanying Datosx 2 acquisition and Datosx rec software to record and reconstruct the tomographies. The scans were performed as fast scans with settings of 100kV, 100 μ A and a voxel size of 21.7 μ m. VGStudioMax3 (Volume Graphics, Heidelberg, Germany) was used to visualize and analyze the resulting depots. To determine the percent of contrast agent that remained in the tissue after injection, a custom region was made around the tissue and the volume of the contrast agent inside this control volume was calculated. This was then divided by the total amount of contrast fluid in the entire image.

Force measurements for ex vivo injections

During ex vivo injection experiments, we measured the forces required to deliver a given dose of liquid into the tissue (Extended Data Fig. 3). We found that delivering an 80 μ L liquid dose through a needle inserted 4 mm into the tissue required 12.1 ± 6.0 N of force, statistically significantly more force than the 5.7 ± 2.7 N of force required to dose the same amount of liquid through a needle inserted 4.5 mm into the tissue ($P=0.009$). While we found that 7.6 ± 3.1 N force was required to inject an 80 μ L liquid dose through a needle inserted 5 mm into the tissue, this was not statistically significantly more than the injection force found for a 4.5 mm needle insertion depth ($P=0.12$). Additionally, the 8.0 ± 4.1 N force required when dosing into the muscularis layer of tissue at a needle insertion depth of 5 mm ($n=6$) was not statistically significantly different from the injection forces required for liquid dosing at this depth overall ($P=0.8$). This suggests that penetration into the muscular layer would not affect the force required to inject a liquid dose and therefore would not limit the delivered dose volume.

Because we found in these experiments that the injection force required was sensitive to the insertion depth, we tested needles with high angle backgrinds. These needles possessed an outlet hole which was smaller in the direction of needle insertion and therefore targeted an insertion depth more specifically. We found that these needles were unable to insert any significant amount of liquid into the tissue even at forces of >50N (Extended Data Fig. 3). Although the plunger was displaced by the tensile strength tester used to measure the force, we saw no contrast dye in the tissue after trying to deliver the dose. These forces instead were due to the compression of the rubber stoppers and other materials used in the dosing mechanism. From these experiments we chose to use a needle with a low angle backgrind in the L-SOMA.

In vivo pharmacokinetics studies

All studies involving animals were approved by and performed in accordance with the Committee on Animal Care at MIT or the Novo Nordisk Ethical Review Council.

To permit delivery of a clinically relevant drug load in an 80 μ L volume, we developed an up-concentrated formulation of unmodified recombinant human insulin at 12.5 mg/mL and an up-concentrated formulation of semaglutide-like inactivated GLP-1 analog at 50 mg/mL. We also increased the concentration of epinephrine in our L-SOMA from a typical formulation of 1:1000 to 1:333. We used a commercially available formulation of 50 mg/mL adalimumab.

The L-SOMA devices used in these pharmacokinetics studies included the needle insertion and drug delivery actuation systems but did not include the needle retraction system.

Epinephrine and adalimumab pharmacokinetic studies were performed at MIT. We administered the API formulation to female Yorkshire swine (Tufts, North Grafton USA). The swine dosed during the Adalimumab studies had a mass between 30 kg to 60 kg, and the swine dosed during the epinephrine study had a mass between 70 to 80 kg. For these studies, we placed the swine on a liquid diet 24 hours before the procedure and fasted the swine overnight. We anesthetized them with intramuscular injections of Telazol (tiletamine/zolazepam) (5 mg/kg),

xylazine (2 mg/kg), and atropine (0.05 mg/kg) and intubated and maintained them on 2-3% isoflurane in oxygen. Epinephrine dosing was performed in one of the three following ways: (1) The animal was dosed intramuscularly with 240 μ L of 1:1000 dilution epinephrine (McKesson Corporation, San Francisco, USA); (2) A total of 240 μ L of 1:1000 dilution epinephrine (McKesson Corporation) was delivered into the stomach via a gastric endoscope, and the gastric endoscope was flushed with up to 60 mL of water to ensure that all of the epinephrine passed into the stomach; (3) An orogastric tube or overtube was placed in the esophagus with guidance of a gastric endoscope and an L-SOMA device was passed through the overtube into the insufflated stomach with the aid of a gastric endoscope. The L-SOMA device then oriented, actuated and delivered an 80 μ L dose of 1:333 epinephrine produced by diluting 15 mg of epinephrine powder (Sigma Aldrich) along with 35 mg of sodium chloride, and 5 mg of sodium metabisulfite in 5 mL water adjusted to a pH between 2-5 using hydrochloric acid. During the epinephrine experiments, the heart rate was monitored continuously beginning 10 minutes before administration of the drug. The blood glucose was also measured every 2.5-10 minutes beginning 10 minutes before the epinephrine dose and continuing until 2 hours after the dose was administered. Blood samples were tested for glucose levels using a OneTouch Ultra glucose monitor by LifeScan Inc. (Miplitas, USA). The t=0 time point for the L-SOMA devices for the blood glucose and heart rate measurements was considered to be the time of device actuation, while the t=0 for the blood plasma concentrations was considered to be the time of device administration. Blood samples were collected in ethylenediaminetetraacetic K3 tubes (Sarstedt, Numbrecht, Germany) and spun down at 2000 Relative Centrifugal Force for 10 minutes. Blood plasma was collected and stored for up to 2 months in a -80 °C freezer. The blood plasma was then tested for the presence of epinephrine using an epinephrine ELISA kit KA1882 from Abnova (Taipei, Taiwan). The baseline epinephrine concentration at time t=0 minutes was subtracted from all of the sample points. If an epinephrine concentration was read out on the ELISA that was below the t=0 concentration, then the concentration was considered 0 ng/mL.

Adalimumab dosing was performed using the same three methods as described above, except during these experiments 80 μ L of Humira® (Abbvie, North Chicago, USA) was delivered. Additionally, adalimumab was dosed

subcutaneously rather than intramuscularly as a control. The prescription version of Humira® used in these experiments possessed an adalimumab concentration of 50 mg/mL. Blood samples were collected in serum separator tubes (Becton Dickinson, Franklin Lakes, USA) for 10 days after the administration of the drug. The samples were spun down at 2000 Relative Centrifugal Force for 15 minutes and the serum was collected and stored for up to 2 months in a -80 °C freezer. The blood serum was then tested for the presence of adalimumab using an adalimumab ELISA kit ab237641 from Abcam (Cambridge, UK).

Insulin and the GLP-1 analog pharmacokinetic studies were performed at Novo Nordisk. We chose to deliver an inactivated semaglutide-like GLP-1 analog rather than semaglutide itself to prevent gastrointestinal side effects in the swine model due to the large dose size and high bioavailability provided as a single dose by the L-SOMA system. The analog used possessed a comparable molecular weight (4 kD) and similar pharmacokinetics to semaglutide. Swine used in the study were fasted overnight. Straw was left in the swine's cage during this time, and this hay was often found in the swine's stomach during the L-SOMA experiments the following day. The thickness of the layer of the gastric fluid and food particles could reach up to the height of the L-SOMA capsule at some points. No animals were excluded from the study, even if there was food left in the stomach. To assess the pharmacokinetic uptake of liquid formulations delivered by the L-SOMA capsule, we administered the drug formulations to Landrace Yorkshire Duroc cross-breed pigs (bodyweight 50-100 kg) (Novo Nordisk, Denmark). The swine model possesses anatomical similarities in its GI tract to humans and this model is widely used in GI tract device evaluation. Importantly the swine model is known for its slow gastric emptying times of >24 hours, and the ability for the L-SOMA to pass through and be excreted by the swine demonstrates that the devices can pass through the gastrointestinal tract even when experiencing slow transit times. No adverse effects were observed during the experiments. For subcutaneous dosing studies, we applied a brief anesthesia using propofol (102 mg/kg BW intravenously) (Rapinivet vet 10/mg/mL; Schering-Plough Animal Health, Ballerup, Denmark). For intragastric studies we used either propofol as above combined with inhalation isoflourane or a combined injection anesthesia where the swine were anesthetized with 0.06 mL/kg BW of (125 mg tiletamine [0.75 mg/kg] and 125 mg zolazepam [0.75 mg/kg],

[Zoletil 50; ChemVet, Silkeborg, Denmark] plus 125 mg, xylazine [0.75 mg/kg] [Narcoxyl vet 20 mg/mL; Intervet, Ballerup, Denmark] plus 125 mg ketamine [0.75 mg/kg] [Ketaminol vet 100 mg/mL; Intervet] + 125 mg butorphanol [0.15 mg/kg] [Torbugesic vet 10 mg/ mL; Scanvet, Fredensborg, Denmark]). Some swine were woken up from anaesthesia immediately after dosing the L-SOMA while some swine were left under anaesthesia for two hours following administration. Animals were supplemented with 1/3 of initial anaesthesia dose every 30 min. L-SOMA devices were dosed via an endoscope and dropped into the stomach. The devices were then allowed to independently actuate. After 2 hours, the devices were removed from the stomach via an endoscope. Of note, one device loaded with insulin actuated before reaching the stomach because the endoscope operator was not able to easily navigate the esophagus of the swine, and this sample removed from the data set. Blood samples were obtained via a central venous line at designated time points, including but not limited to every 15 minutes for the first two hours and every 30 minutes for hours 2-4. Additionally, blood samples were taken for up to 3 days after administration. Blood samples were immediately tested for glucose levels using a OneTouch Ultra glucose monitor by LifeScan Inc. (Milpitas, USA). Also, blood samples containing insulin and the GLP-1 analog were collected in ethylenediaminetetraacetic K3 tubes (Sarstedt, Numbrecht, Germany). These blood samples were analyzed via an AlphaLISA developed by Novo Nordisk. These AlphaLISA assays are specific to the given molecule and do not cross react with other endogenous molecules.

One animal dosed with human insulin showed a plasma insulin level of 41.6 pM at t=0. This may have been due to a sample contamination during the assay readout. This animal's plasma glucose rose to a peak of 136 pM at 45 minutes and maintained a sustained plasma insulin level higher than the time 0 value throughout the whole sampling period, suggesting that insulin was delivered in this swine using the L-SOMA. However, because of the potential contamination, we removed the data from the dataset in figure 3 and from the bioavailability calculation. Although the swine dosed were partially fasted, some swine contained a layer of gastric fluid and food particulate in their stomachs measuring several millimeters. In these swine, the L-SOMAs were able to displace the food layer,

insert their needles into the tissue, and still deliver the drug load. Of note, one device loaded with GLP-1 analog and one device loaded with insulin actuated in the stomach, but the swine showed no systemic uptake. This was likely due to the drug formulation not reaching the gastric submucosa or leaking out into the lumen. Additionally, one insulin loaded device did not actuate at all, likely stemming from an error during manual assembly.

In vivo Oral Dosage Studies

We orally dosed unsedated swine and beagle dogs with a single SOMA or L-SOMA device each, and the animals swallowed the devices naturally. Each device was placed at the back of the mouth and 10 mL water was provided to facilitate swallowing the device. We used radiograph imaging to track the device as it passed through the gastrointestinal tract.

Stability Studies

Liquid formulations of 12.5 mg/mL insulin and 50 mg/mL semaglutide were placed into either an L-SOMA device or a glass vial. These filled devices and cartridges were then placed in a climate chamber maintained at 40°C and 75% relative humidity for 2 weeks. The L-SOMA devices in which the insulin was tested were not washed before loading the drug into the capsule, while the devices loaded with semaglutide were washed before loading the drug. The washing step may have an effect on the stability of the drug in the device. Once retrieved, the formulations were examined for high molecular weight protein content and purity loss via high performance liquid chromatography.

We observed that the purity loss and high molecular weight protein formation for the formulations placed in the L-SOMA system was greater than for formulations placed in a glass vial after undergoing two weeks in a 40°C and 75% relative humidity environment (Extended Data Fig. 1). Additionally, the purity loss for the liquid formulation was higher than the purity loss for the solid formulation we previously reported using the SOMA system²¹. The initial glass vial studies provide evidence that it is possible to maintain our custom designed drug formulations at a stability that meets commercial stability requirement guidelines; however, adjustments to the L-SOMA storage system which make it more similar in chemical composition and sterility to the glass vial storage system may be

required to ensure long-term stability of the filled drug. Additionally, it should be noted that the formulations used in this study contained high concentrations of drug, are not the marketed formulations of the compounds, and have not yet been optimized in terms of formulation stability to accommodate the high concentration. Further formulation optimization may also increase the stability of drug formulation loaded in the L-SOMA.

Bioavailability Calculations

Individual plasma concentration-time profiles were analyzed by a non-compartmental model in WinNonlin Phoenix version 6.3 (Pharsight Inc., Mountain View, CA, USA) and the resulting terminal half-lives were determined for IV, SC, and PO dosing. For PO and S.C. studies the absolute bioavailability (F) was calculated; the dose-corrected AUC was calculated after both oral administration and intravenous administration to swine, and specifically F% was calculated as AUC/Dpo divided by AUC/Div times 100. For inactivated semaglutide-like GLP-1, the time from 0-72 hr was used for calculating AUC, thus the pharmacokinetic profile was not extrapolated to infinity due the relatively short sampling compared to the $t_{1/2}$ and the associated uncertainty extrapolating to infinity when the sampling time only constitutes 2x $t_{1/2}$. For insulin, the AUC was extrapolated to infinity using linear regression. One animal did not have exposure of inactivated semaglutide-like GLP-1, and thus the absolute bioavailability was indicated as "0" for this animal.

Clinical Feasibility Assessment

The L-SOMA capsule facilitates a rapid pharmacokinetic uptake within minutes after administration and possesses a loading capacity of up to at least 4 mg of bioavailable drug, enabling the compatibility of this capsule with a new set of medications that could not previously be orally delivered. For adalimumab, taking the 4 mg pill daily would deliver a total dose 56 mg over the course of a two-week period compared to the prescribed subcutaneous injection dose of 40 mg once every two weeks. Higher drug loads may be feasible depending on the solubility of the selected compound, and the company Elektrofi recently demonstrated a method to create an injectable formulation with a monoclonal antibody concentration up to 500 mg/mL³⁹. That would translate to a dose of 40 mg per L-SOMA. In

order to deliver high viscosity fluids that arise from highly concentrated drug formulations, the injection spring and needle gauge size can be strengthened and widened, respectively, to accommodate injection. Furthermore, the fluid path into the needle lumen can be further optimized to reduce fluid shear stress. The other drugs tested in this study all are prescribed at doses below 4 mg per injection. In fact, the absorption and bioavailability of long acting GLP-1 dosed via the L-SOMA suggest that the L-SOMA system may enable once weekly dosing of compounds with similar dose requirements and a long systemic $t_{1/2}$. For potent, rapid acting drugs, such as insulin, it will be important to develop dosing and drug loading systems that allow the user to deliver doses specific to their individual needs. This could be facilitated through prefilled pills with different dose sizes or through at home filling stations that allow for customizable dose sizes. While the ability to deliver epinephrine for anaphylaxis using the L-SOMA may be hindered by swallowing difficulties in serious cases, the capsule could still be used to deliver the drug for slower onset allergic reaction. Additionally, the use of epinephrine in the L-SOMA device demonstrates the ability to deliver small molecule drugs which require parenteral administration. Poorly soluble small molecule drugs which demonstrate low systemic uptake⁴⁰ may also be suitable candidates for the L-SOMA system. The broad-ranging applicability of the L-SOMA means that it is possible to load the capsule with any liquid formulation including small molecule or macromolecule drugs; albeit reformulation and up concentration may be necessary to reach the required therapeutic dose for a given drug. Furthermore, investigation on the potential of applying the depot sites for controlled prolonged release may be of interest across a range of clinical applications.

Statistical Analysis

No data was excluded from the analysis. Unpaired Student's t-tests and one-way ANOVA with Tukey's multiple comparisons tests were performed using Prism Version 8.3 (GraphPad) or Microsoft Excel (Microsoft). A value of $P < 0.05$ was considered statistically significant. Figure captions and text describe the number of replicates used in each study. Figure captions define the center line and error bars present in the plots.

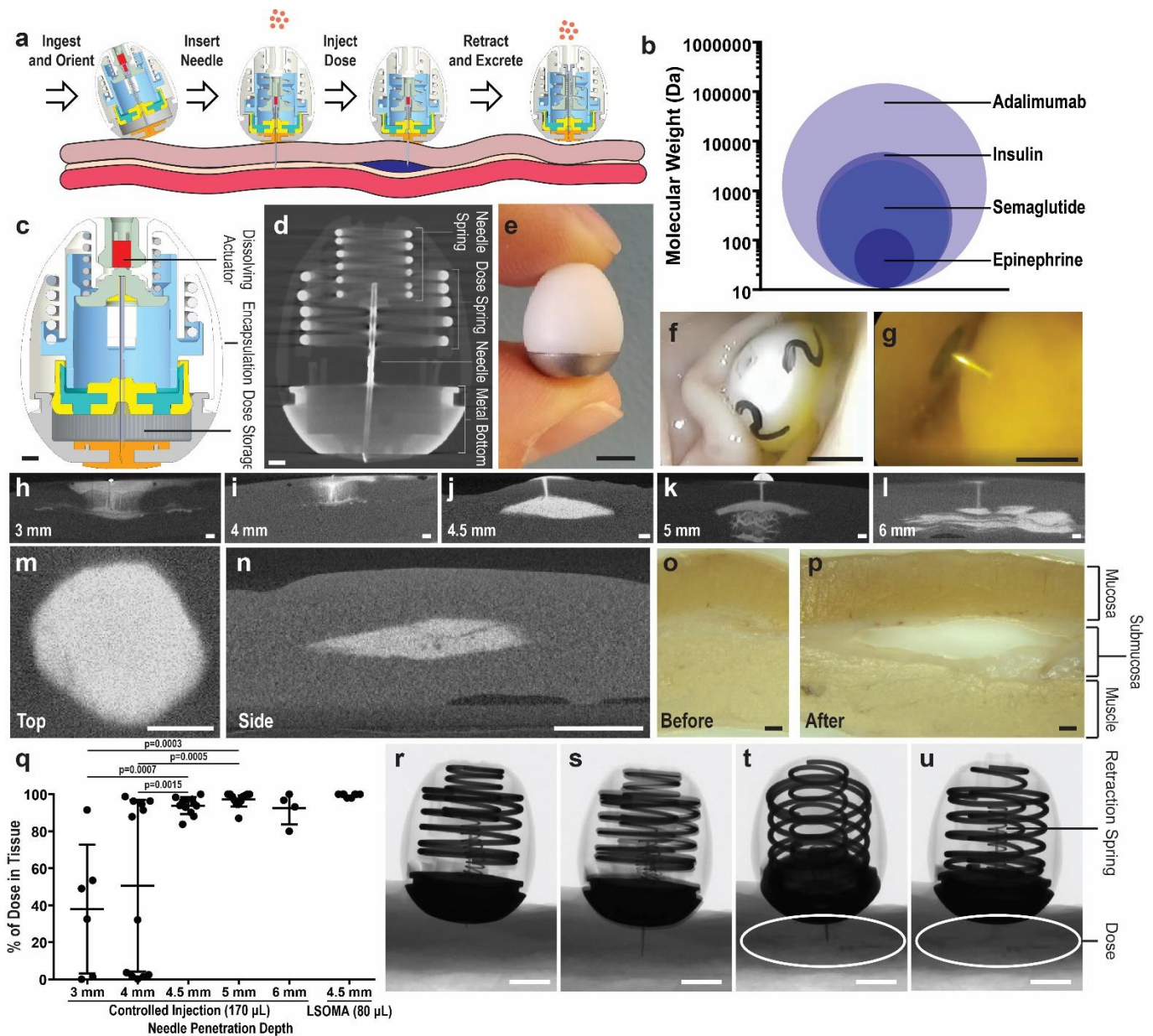


Figure 1: An oral pill for liquid drug injections into the gastric submucosa. (a) Device timeline. (b) Molecular weight of drugs delivered using L-SOMA. (c) CAD design, (d) Micro-CT scan, and (e) photo of non-retracting device before actuation. (f) In vivo actuation of L-SOMA and (g) close-up of needle injection site. (h-l) Representative images of contrast dye which remained in ex vivo swine stomach tissue after 170 μ L injection. (m) Top and (n) side view of an 80 μ L depot of contrast dye injected by an L-SOMA capsule with a needle insertion length of 4.5 mm. (o) Microtome image of fixed swine stomach tissue before and (p) after an injection with the L-SOMA. (q) Percent of contrast dye which remained in tissue after injection. The value was calculated using 3D reconstructions of Micro-CT images (Mean \pm SD. Ordinary one-way ANOVA with Tukey's multiple comparisons test). (r-u) Micro-CT images of an L-SOMA (s) actuating into ex vivo swine stomach tissue, (t) injecting contrast dye, and (u) retracting its needle.

Images are clipped from Supplementary video S1. (b, c, h-l, o-p: Scale Bar = 1 mm; d, f, g, m, n, r-u: Scale Bar = 5 mm) (n=X technical replicates [3 mm: n=6, 4 mm: n=12; 4.5 mm: n=12; 5 mm n=12; 6 mm: n=4; L-SOMA: n=8]).

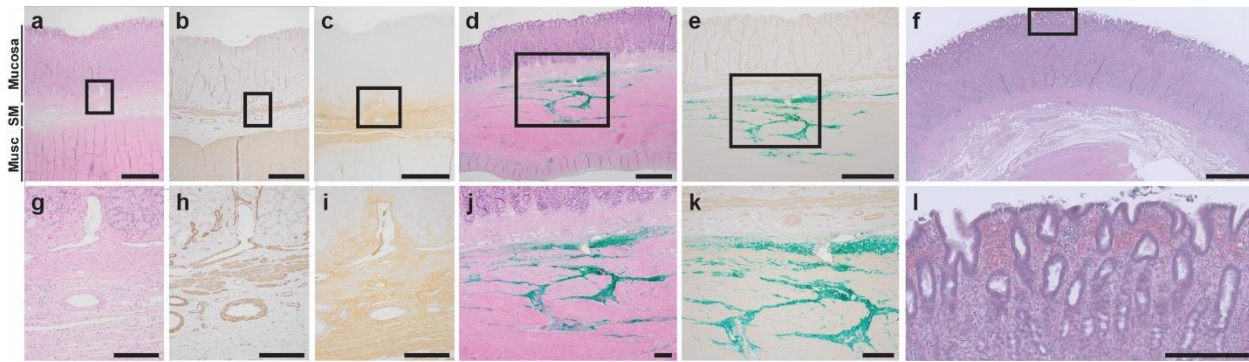


Figure 2: Histology after L-SOMA capsule administration. (a-c) Histology of ex vivo swine stomach after an LSOMA insulin injection using (a) a hematoxylin and eosin stain, (b) an immunohistochemistry stain against alpha smooth muscle actin, or (c) an immunohistochemistry stain against insulin. (d-e) Histology of in vivo swine stomach immediately following L-SOMA administration of green dye using (d) a hematoxylin and eosin stain or (e) an immunohistochemistry stain against alpha smooth muscle actin. (f) Histology sample from an injection site of a swine dosed with multiple L-SOMA injections over three days. Image shows a minimal acute superficial hemorrhage with intact epithelial lining. This area was likely the location of the injection that occurred six hours prior to euthanasia. No other macroscopic abnormalities were found in the stomach from devices fired more than one day before euthanasia. (g-l) Zoomed histology images respectively corresponding to the boxed section of the images a-e. SM=Submucosa. Musc= Outer Muscle Layer. (a-f: Scale Bar = 1 mm. g-l: Scale bar = 250 μ m). Example images are from one of three animal replicates.

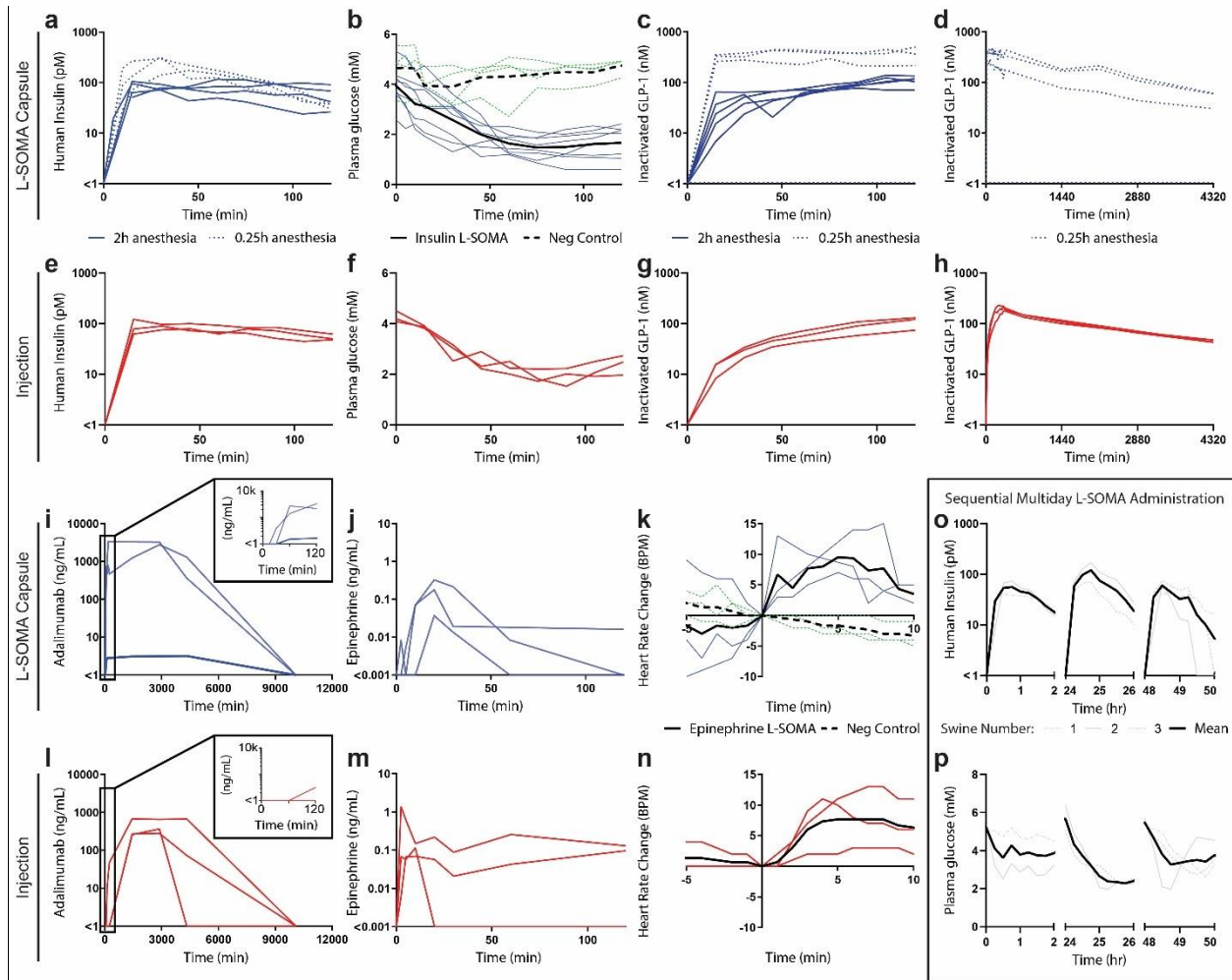
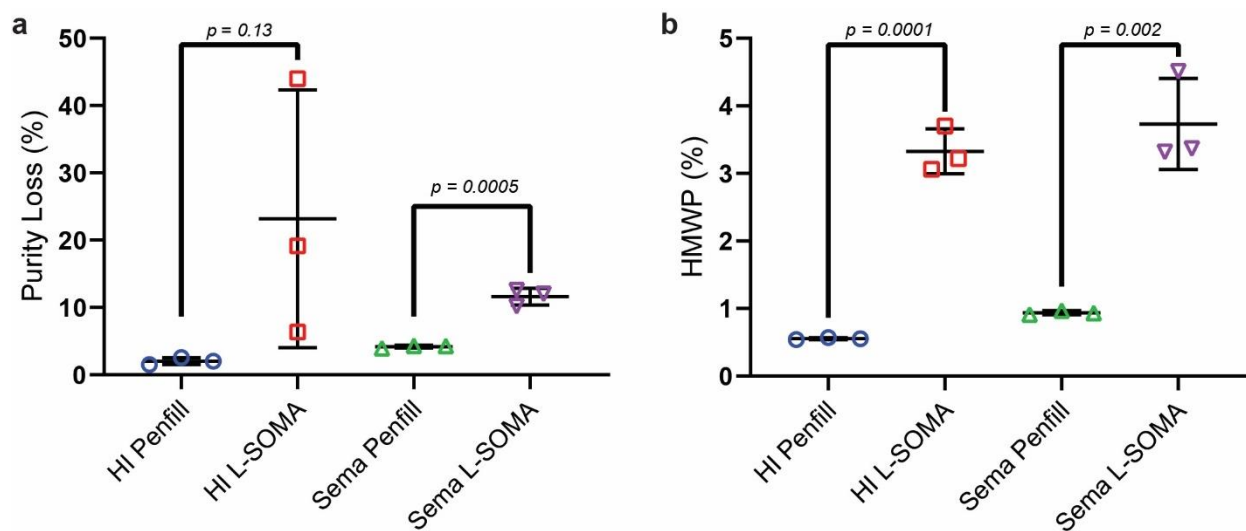
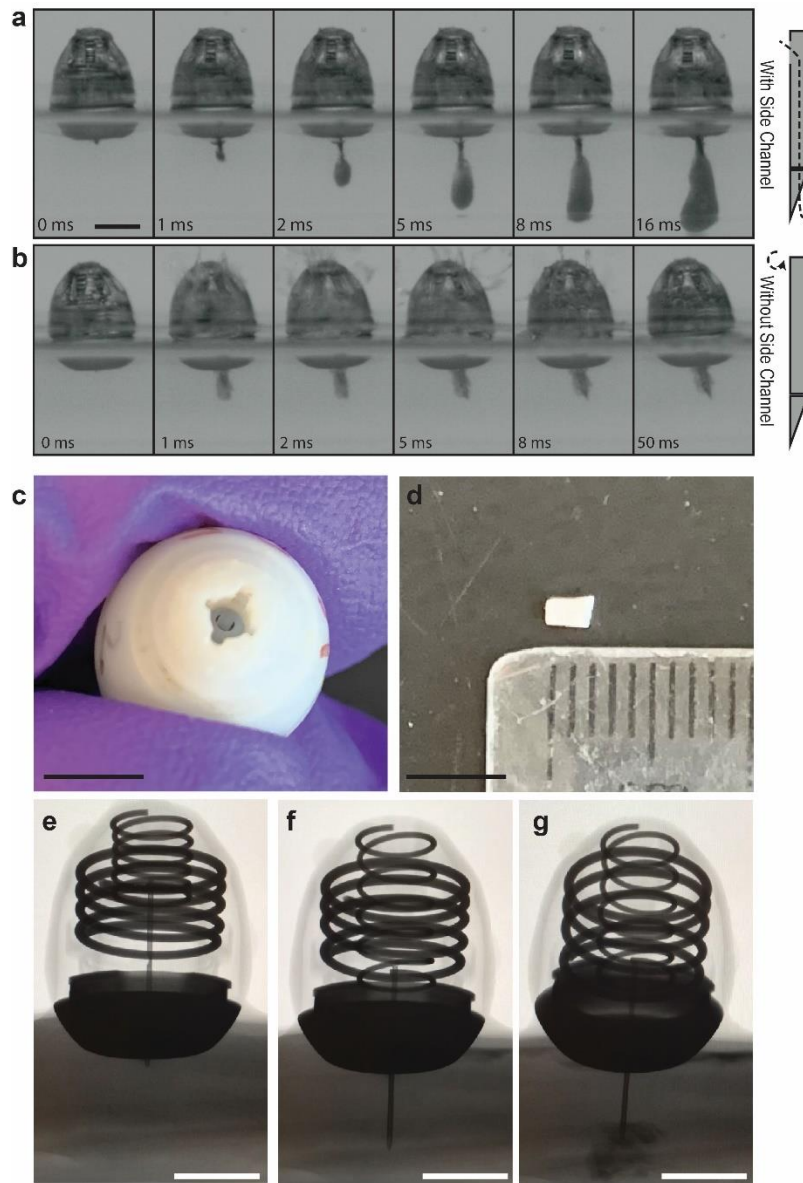


Figure 3: Single and multiday oral delivery of monoclonal antibodies, peptides, and small molecule drugs in swine. (a) Blood plasma human insulin and (b) glucose levels after dosing an L-SOMA capsule containing 4 International Units (IU) (0.14 mg) of recombinant human insulin (n=7, black line=mean). The negative control for plasma glucose is the L-SOMA delivery of 4 mg inactivated GLP-1 analog (n=4 animal replicates). (c-d) Blood plasma levels of inactivated GLP-1 analog after dosing an L-SOMA containing 4 mg of inactivated GLP-1 analog. (n=9). Swine receiving anesthesia only during L-SOMA administration (0.25h) and swine receiving anesthesia for two hours after administration are noted on the graphs. (e) Blood plasma human insulin and (f) glucose levels after subcutaneously dosing 4 IU of recombinant human insulin (n=3). (g-h) Blood plasma levels of inactivated GLP-1 analog after subcutaneously dosing 4 mg of inactivated GLP-1 analog. (n=3). (i) Blood serum levels of adalimumab after dosing an L-SOMA capsule containing 4 mg of adalimumab (n=3). (j) Blood plasma levels of epinephrine and (k) associated heart rate change after dosing an L-SOMA capsule containing 0.24 mg epinephrine (n=3, black line=mean). The negative control for heart rate change is an endoscopic gavage dosing containing 0.24 mg epinephrine (n=3). (l) Blood serum adalimumab levels after subcutaneous dosing of 4 mg adalimumab (n=3). (m) Blood plasma epinephrine levels and (n) associated heart rate change after intramuscular dosing of 0.24 mg of epinephrine (n=3, black line=mean). For the heart rate change data, time 0 corresponds to the time of device actuation or injection. For all other data, time 0 corresponds to the time of device administration. (o) Sequential multiday administration of recombinant human insulin to three swine using the L-SOMA demonstrates consistent systemic drug exposures and (p) plasma glucose lowering responses. On day 1, a device did not actuate in swine 3, and on day 2, a device

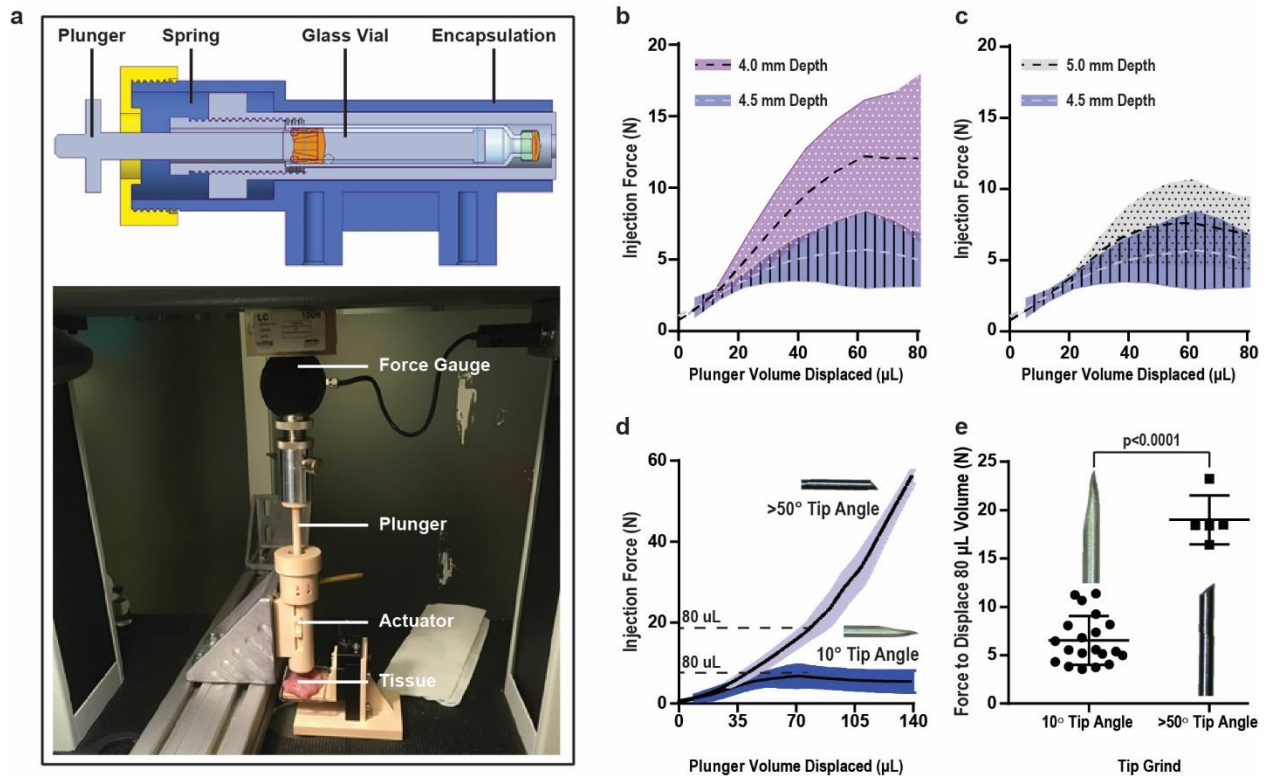
actuated in swine 1 but did not systemically deliver drug. Solid black lines represent the average for a given administration group. All other lines represent the dosing of a different animal or the same animal dosed at least three weeks apart.



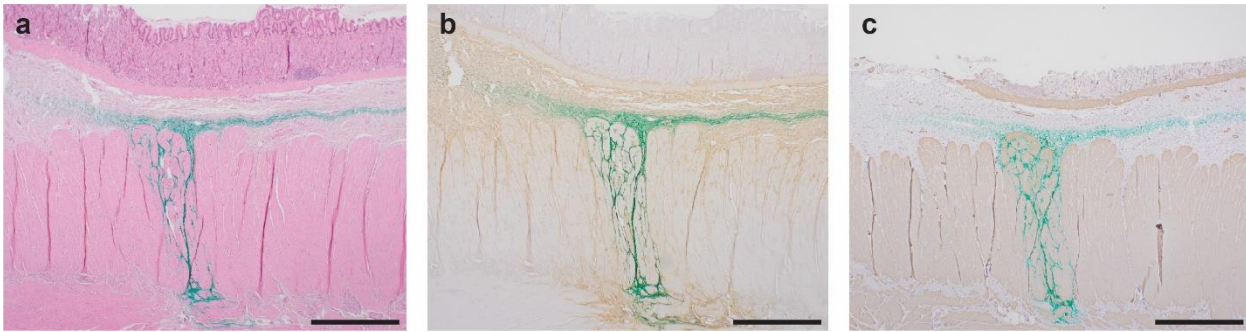
Extended Data Fig. 1: Liquid Formulation Stability. Human Insulin (HI) concentrated to 12.5 mg/mL and a semaglutide (Sema) exploratory formulation concentrated to 50 mg/mL were placed inside of either an L-SOMA or a glass vial and were subjected to a 40°C and 75% relative humidity environment for two weeks. (a) Purity loss and (b) high molecular weight protein (HMWP) formation were then measured. (Mean ± SD, n=3 device replicates; Unpaired t test).



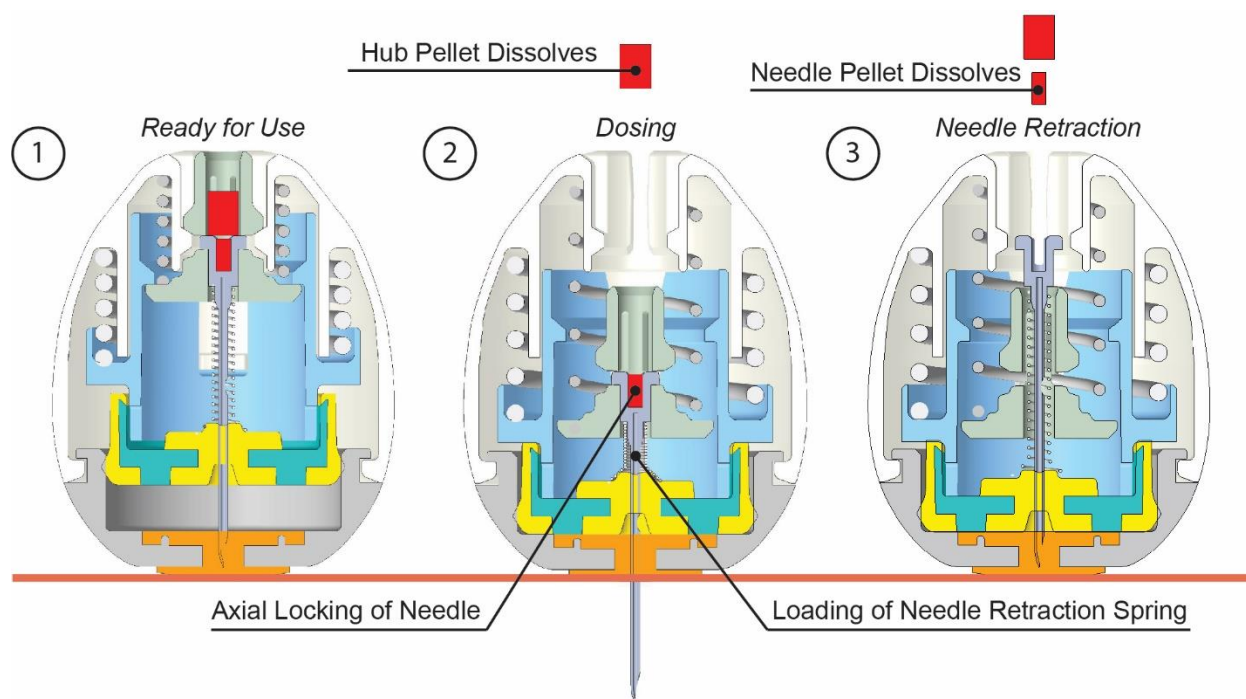
Extended Data Fig. 2: L-SOMA needle injection images. (a) High speed photography of an initial prototype L-SOMA device with a 21 G needle actuating into 0.3% agarose gel demonstrated that all of the liquid exits through the needle tip and none of the liquid exits through the bottom membrane. (Images are from one of n=3 technical replicates). (b) No drug is delivered if the needle lacks a side channel (Images are from one of n=3 technical replicates). Prototypes used during future ex vivo and in vivo studies employed a 32 G needle rather than a 21 G needle. (n=3 technical replicates). (c) Hole on top of the L-SOMA device allows access to the (d) dissolving pellet, which actuates the needle injection. (e-g) Sequential MicroCT images of a non-retracting L-SOMA delivering contrast dye into ex vivo swine tissue. (Images are from one of n=8 technical replicates). Scales Bars = 5 mm.



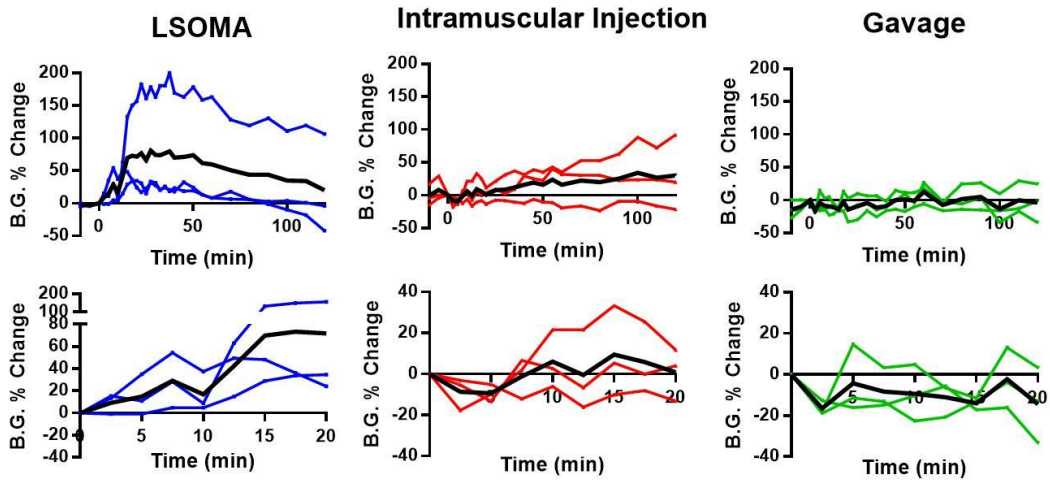
Extended Data Fig. 3: Injection test mechanism setup and ex vivo injection force calculations. (a) (Top) Computer aided design of the custom actuation mechanism used to insert a needle a controlled distance and inject an exact amount of fluid. (Bottom) Experimental setup of controlled injection studies. The texture analyzer pushes down on the plunger which causes the liquid to inject into the swine stomach tissue below. (b-c) The force required to inject a depot into ex vivo swine stomach tissue at a given needle insertion depth. (Mean \pm SD; 4 mm: n=11 ; 4.5 mm: n=9 ; 5 mm: n=18). (d-e) The force required to inject a depot into ex vivo swine stomach tissue using a needle with a 10° bevel and a bevel of >50°. (Mean \pm SD; 10°: n=20; >50°: n=5; Unpaired t test).



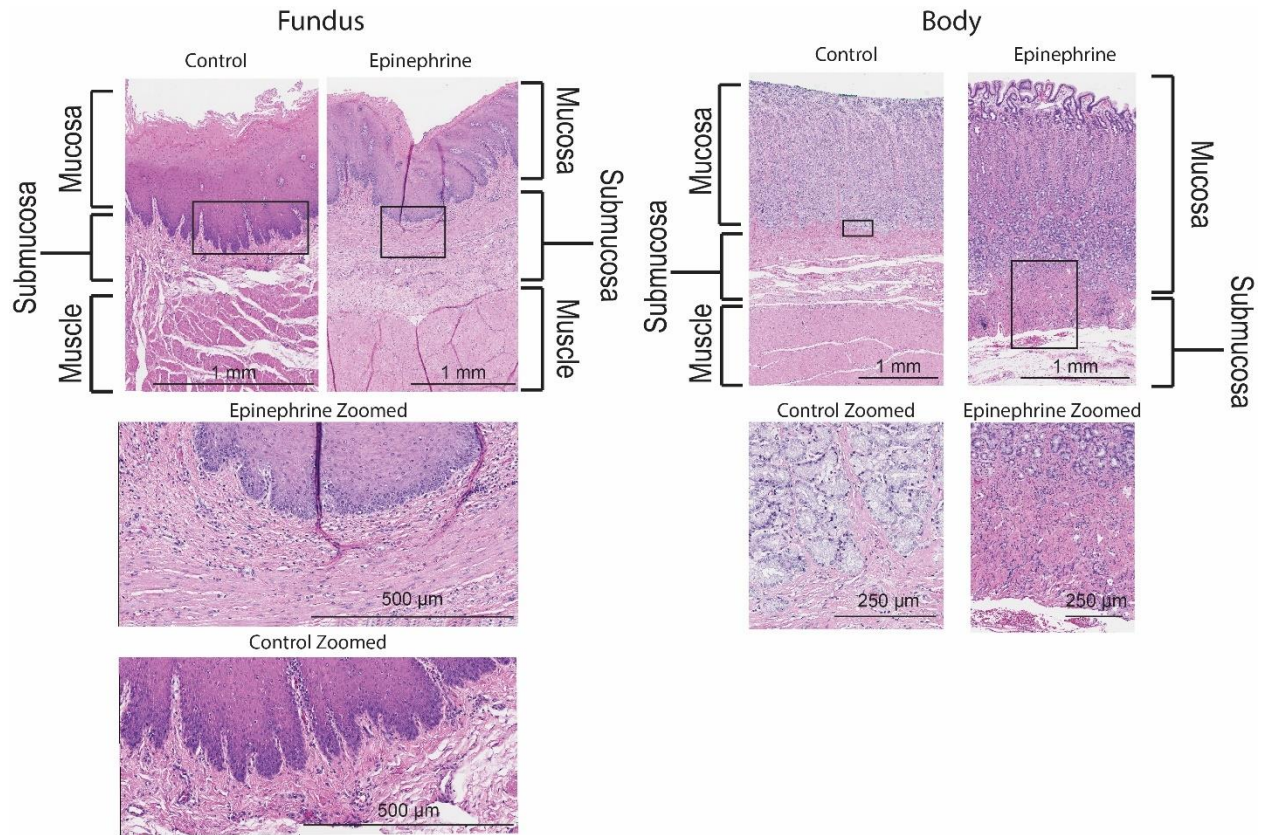
Extended Data Fig. 4: Dog ex vivo histology from L-SOMA injection. Histology of ex vivo dog stomach after an L-SOMA insulin injection using a (a) hematoxylin and eosin stain, (b) an immunohistochemistry stain against insulin, (c) or an immunohistochemistry stain against smooth muscle actin. These are example images from one of 3 replicates. Scale bar = 1 mm.



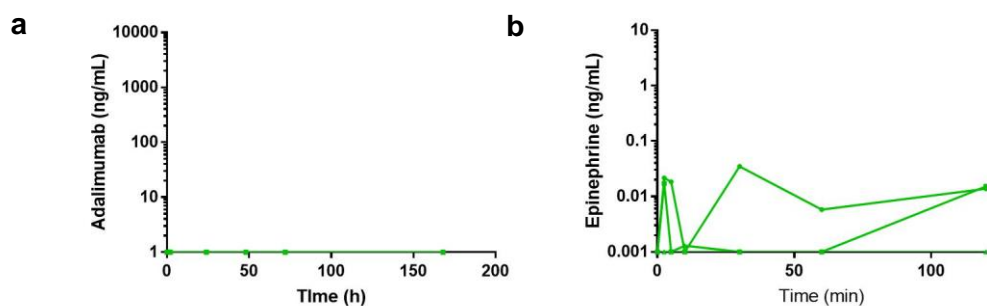
Extended Data Fig. 5: L-SOMA needle retraction mechanism design. The device first actuates after the hub pellet (red) dissolves and allows the latching mechanism at the top of the pill to release. The retraction spring, located axially around the needle shaft, compresses after the first stage of actuation due to the inherent movement of the needle during injection. The dissolution of the second pellet, which is exposed only after the first pellet dissolves, frees the spring to expand and draw the needle back into the capsule.



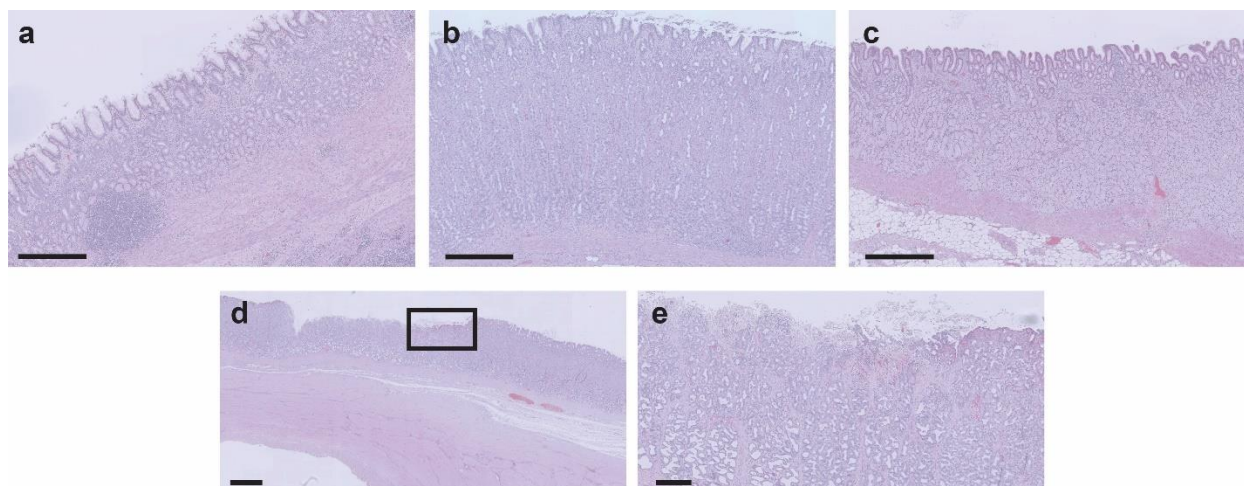
Extended Data Fig. 6: Blood glucose change in swine after 0.24 mg epinephrine injection. Colored lines represent individual swine profiles and black lines represent the mean values.



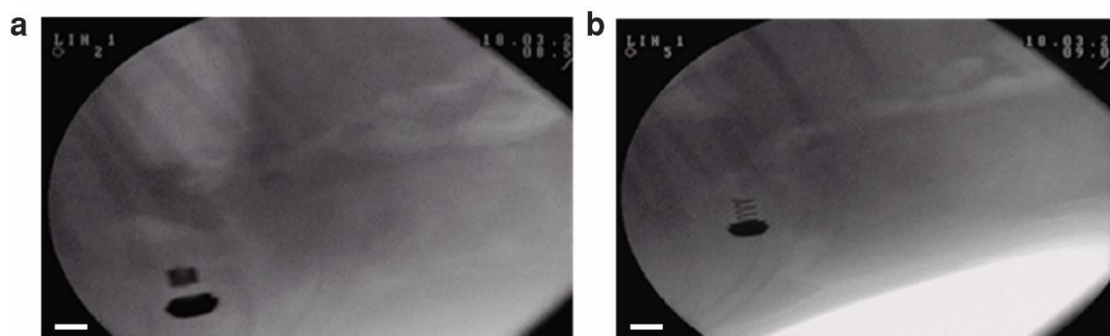
Extended Data Fig. 7: In vivo swine histology after L-SOMA epinephrine injection. Hematoxylin and eosin stain histology of swine stomach hours after L-SOMA injection. L-SOMA devices were injected in the fundus or body of the stomachs. An increase in cellularity is seen between the control and the experimental tissues, but this variability is expected in tissue locations with rapidly dividing cells. Moreover, the regular injection of epinephrine in the stomach during endoscopy supports the safety of intermittent administration of this drug in this location. The control histology is of swine stomach tissue not dosed with any device. These are example images from one of three animal replicates.



Extended Data Fig. 8: Pharmacokinetics of gavage dosed epinephrine and adalimumab. Dissolved (a) adalimumab (4 mg) or (b) epinephrine (0.24 mg) were dosed through an endoscope into the lumen of swine stomachs (n=3 animal replicates).



Extended Data Fig. 9: Histology taken from swine dosed multiple times with L-SOMAs over three days. (a-c) Three samples were collected according to standard histopathological procedures representing the (a) cardia, the (b) fundic, and the (c) pyloric region. No treatment related findings were observed in these standard samples in any of the three swine. (d) Histology from a minimal focal lesion from the fundic region of one of the three swine. The image shows an acute minimal erosion with sloughing of epithelial cells and peripheral acute hemorrhage. This injury is most likely a mechanical trauma caused by the endoscope when dosing the animal and is not a direct effect of the intended L-SOMA dosing. (e) Zoomed in image of “d”. (a-c: Scale Bar = 500 μ m; d: Scale Bar = 1 mm.; e: Scale Bar = 250 μ m).



Extended Data Fig. 10: SOMA actuation in dog stomach after oral dosing in an awake dog. A radiograph of the SOMA device (a) before and (b) after actuating in the gastric cavity. Note the extension of the spring in the right panel. Scale Bar = 5 mm.

Supplementary Materials for

Ingestible robotic capsule injectors for oral delivery of systemic monoclonal antibodies, peptides and small molecules

Authors: Alex Abramson^{1,*,5}, Morten Revsgaard Frederiksen^{2,#,5}, Andreas Vegge^{3,5}, Brian Jensen², Mette Poulsen², Brian Mouridsen², Mikkel Oliver Jespersen², Rikke Kaae Kirk³, Jesper Windum², František Hubálek⁴, Jorrit J. Water⁴, Johannes Fels⁴, Stefán B Gunnarsson⁴, Adam Bohr⁴, Ellen Marie Straarup³, Mikkel Wennemoes Hvitfeld Ley², Xiaoya Lu^{1,8}, Jacob Wainer^{1,%}, Joy Collins¹, Siddhartha Tamang¹, Keiko Ishida^{1,9}, Alison Hayward^{1,9}, Peter Herskind², Stephen T. Buckley⁴, Niclas Roxhed^{1,6}, Robert Langer^{1,5,7}, Ulrik Rahbek^{4*}, Giovanni Traverso^{1,8,9*}

Affiliations:

¹Department of Chemical Engineering and David H. Koch Institute for Integrative Cancer Research, Massachusetts Institute of Technology, Cambridge, MA 02139

²Devices and Delivery Solutions, Novo Nordisk A/S, Hilleroed, Denmark

³Global Drug Discovery, Novo Nordisk A/S, Maaloev, Denmark

⁴Global Research Technologies, Novo Nordisk A/S, Maaloev, Denmark

⁵Institute for Medical Engineering and Science, Massachusetts Institute of Technology, Cambridge, MA 02139

⁶Department of Micro and Nanosystems, KTH Royal Institute of Technology, Stockholm, Sweden.

⁷Media Lab, Massachusetts Institute of Technology, Cambridge, MA 02139

⁸Department of Mechanical Engineering, Massachusetts Institute of Technology, Cambridge, MA 02139

⁹Division of Gastroenterology, Brigham and Women's Hospital, Harvard Medical School, Boston, MA 02115

*Correspondence to: ulyr@novonordisk.com, cgt20@mit.edu

Supplementary Material for this manuscript includes the following:

Supplementary Video S1: Ex vivo actuation of a retractable Liquid SOMA capsule captured using MicroCT.

Supplementary Video S2: In vivo delivery of radio-opaque contrast dye to the stomach wall using a Liquid SOMA capsule.

Supplementary Data 1: Calculations of bioavailability in swine for L-SOMA dosed insulin and GLP-1.

Supplementary Data 2: Actuation times of L-SOMA after delivery in swine.